Measurement Report: An Exploratory Study of Fluorescence and CCN Activity of Urban Aerosols in San Juan, Puerto Rico

Bighnaraj Sarangi [1*], Darrel Baumgardner[3], Benjamin Bolaños-Rosero[4] and Olga L. Mayol-Bracero[1, 2]

[1]Department of Environmental Sciences, University of Puerto Rico - Río Piedras Campus, San Juan, Puerto Rico, USA
[2] Now at Environment and Climate Sciences Department, Brookhaven National Laboratory, Upton, New York, USA
[3] Droplet Measurement Technologies LLC, Longmont, Colorado, USA
[4]Department of Microbiology, School of Medicine, University of Puerto Rico - Medical Sciences Campus, San Juan, Puerto Rico, USA

(*Correspondence: bighnarajsarangi1986@gmail.com)

Abstract

Many atmospheric aerosols are cloud condensation nuclei (CCN), capable of activating as cloud droplets when the relative humidity exceeds 100%.~~Many types of atmospheric aerosols cloud condensation nuclei (CCN) capable of activating as cloud droplets~~. Some primary biological aerosol particles (PBAP), such as plant spores, pollen, or bacteria, have been identified as such CCN. Urban environments are a source of these bioaerosols, those that are naturally produced by the local flora, or are transported from surrounding regions, and others that are a result of human activities. In the latter case, open sewage, uncovered garbage, mold or other products of such activities can be a source of PBAPs. There have been relatively few studies, especially in the tropics, where PBAPs and CCN have been simultaneously studied to establish a causal link between the two. The metropolis of San Juan, Puerto Rico is one such urban area with a population of 2,448,000 people (as of 2020). To better understand the fluorescent characteristics and cloud forming efficiency of aerosols in this region, measurements with a Wideband Integrated Bioaerosol Spectrometer (WIBS), a condensing nuclei (CN) counter, and

a CCN spectrometer were made at the University of Puerto Rico – Rio Piedras Campus. Results show that the CCN/CN activation ratio and the fraction of fluorescing aerosol particles (FAP) have repetitive daily trends when the FAP fraction is positively correlated with relative humidity and negatively correlated with wind speed, consistent with previous studies of fungi spores collected on substrates.

The results from this pilot study highlight the capabilities of ultraviolet-induced fluorescence (UV-IF) measurements for characterizing the properties of FAP as they relate to daily evolution of PBAPs. The use of multiple excitation and emission wavelengths, along with shape detection, allows the differentiation of different PBAP types. These measurements, evaluated with respect to previous, substrate-based analysis of the local fungal and pollen spores, have established a starting database of measurements that future, longer term studies will build upon.

1 Introduction:

The formation and evolution of clouds over the tropical island of Puerto Rico have been studied over the course of many years, primarily with respect to the sources of cloud condensation nuclei (CCN). Puerto Rico has been the site of these studies because of its fair-weather, maritime flow and mostly clean atmosphere that leads to a mountaintop cloud that forms quite frequently throughout the year and can persist for several days (Allan et al., 2008; Gioda et al., 2013; Spiegel et al., 2014; Valle-Díaz, et al., 2016; Raga et al., 2016; Torres Delgado, 2021). In addition to the clean, maritime sources, the cloud studies have also identified particles produced from upwind urban areas, both on the island of Puerto Rico as well as islands to the east, where vehicular and ~~other~~ industrial emissions produced particles with organic carbon and sulfates (Allan et al., 2008). Apart from this, clouds and rainwater in this region are influenced by long-range transported natural aerosols. African dust is also potentially an important source of CCN, although the results are not conclusive as to how much cloud properties differ in the presence of these particles (Spiegel et al., 2014; Valle-Díaz, et al., 2016; Raga et al., 2016; Torres Delgado, 2021).

Airborne, primary biological aerosol particles (PBAP) are an important type of aerosol in the tropics (Gabey et al., 2010,2013; Stanley et al., 2011) that can encompass viruses (0.01-0.3µm), pollen (5-100 µm), bacteria and bacteria agglomerates (0.1-10 µm), and fungal spores (1-30 µm) as well as mechanically formed particles, such as dead tissue and plant debris (Finnelly et al., 2017). Furthermore, there is evidence that PBAP may influence the hydrological cycle and climate by initiating the ice nucleation process or acting as giant CCN (Möhler et al., 2007; Pope, 2010). Although bioaerosols contribute a small fraction (50 Tg yr^{-1}) of the total natural global emissions (~2900-13000 Tg yr^{-1}) (Hoose et al., 2010; Stocker et al., 2013). However, their mass and number concentrations are site specific and greatly vary depending upon the location and climatic condition (references therein Zhang et al., 2021). In terrestrial ecosystems, bioaerosols constitute a major fraction of total aerosol load. As far as urban and rural atmosphere are concern, bioaerosols of size greater than ~1 µm may account for around 30% (references therein Fröhlich-Nowoisky et al., 2016). There is evidence where bioaerosol may constitute a significant fraction (5-50%) in the urban air (Jaenicke, 2005). Upon emission

Formatted: Space After: Auto

from the biosphere, PBAP undergoes various physico-chemical changes (coagulation, photooxidation, surface coating, etc.) and are removed through dry and wet deposition. The reference to giant CCN has now been expanded upon to explain that giant CCN play a special role in precipitation development because they can form larger droplets that more easily collide and coalesce to form raindrops. Hence, although small in number concentration they make up for in their size and capacity to contribute to early precipitation development. In general, biological aerosol particles, until recently, have received less attention in the atmospheric science community for lack of appropriate equipment and the associated measurements are expensive, labor intensive and often difficult to interpret (Cziczo et al., 2006; Drewnick et al., 2008).

Puerto Rico is characterized by tropical climate, urban land cover and use, moist soils, unique topography, and dense vegetation. These factors, associated with the easterly trade winds from the East, could influence the concentration of airborne particles, for examples, organic particles, viruses, bacteria, fungi, pollen, etc. (Velázquez-Lozada et al. 2006). Nevertheless, meteorological variables (high humidity and wind speed) are also the important factors, influencing the airborne particle population in the tropics, including rainy seasons. There are various sources of particulate matter degrading the air quality of Puerto Rico, i.e., from industrial activities, anthropogenic inputs, African temperatures dust storms and volcanic eruptions. The urban areas of Puerto Rico are considered developed with industrial growth, most of which is related to pharmaceutical and power generation plant. The power generation plants are responsible for releasing millions of pounds of air pollutant annually (Torro-Heredia et al., 2020). Data show that a large number of organic compounds (e.g., n-alkanes, esters, phthalates, siloxanes, and other) including plasticizer released into the atmosphere which could pose major health threat in this area (Torro-Heredia et al., 2020). Puerto Rico has abundant plant life, e.g., a wide variety of trees, flowers, mosses and other types of flora; hence, an open question is if fungal or pollen spores produced from these plants might serve as CCN. The bioaerosol population in Puerto Rico, and in particular in the capital city of San Juan, has been studied extensively using analysis of substrates samples (Quintero et al., 2010; Rivera-Mariani et al., 2011; Rivera-Mariani et al., 2020). The objective of the majority of these studies has been to evaluate the health effects of fungal and pollen spores on the local population (Quintero et al., 2010; Rivera-Mariani et al., 2011; Ortiz-Martínez et al., 2015; Rivera-Mariani et al., 2020). The studies by Quintero et al (2010) are particularly interesting with respect to the investigation reported here because they classified a wide variety of fungal and pollen spores

Formatted: Space After: 0 pt

that were the most responsible for respiratory ailments of residents of San Juan. In addition, they could link the relative concentration of these spores to meteorological factors (e.g., relative humidity and wind speed). Hence, given that their studies indicated that bioaerosols are not only produced in large quantities throughout the year, and highly correlated to local meteorology, it is reasonable to investigate if these types of bioaerosols might also be correlated with CCN measurements if such particles are hygroscopic and can easily form water droplets under the right conditions.

Prior to embarking on a longer-term project that will evaluate PBAPs and CCN under a wide range of conditions, a pilot study was designed to conduct an exploratory investigation of the properties of bioaerosols and CCN during September 2019. September was selected because not only did the Quintero et al. (2010) results show that this time of the year is when peak concentrations of spores are found, it is also a month of frequent cloud formation.

In order to identify the PBAP and investigate their potential sources, we used a realtime, particle by particle approach rather than a methodology that requires capturing particles for offline analysis. There has been considerable progress made in the development of technologies based on the working principle of ultraviolet light-induced fluorescence (UV-LIF) (Ho, 1999; Huffman and Santarpia, 2017). The Wideband Integrated Bioaerosol Spectrometer (WIBS) and the Ultraviolet Aerodynamic Particle Sizer (UV-APS) are examples of instruments that can detect PBAP by their fluorescence, in real time, particle by particle, over a wide size range (Savage et al., 2017). The WIBS and the UV-APS have been used in atmospheric bioaerosol studies such as ice nucleation activity of bioaerosol (Twohy et al., 2016), measurement of atmospheric fungal spore concentrations (Gosselin et al., 2016), and investigation of long-range transported bioaerosol in the tropics (Gabey et al., 2010; Whitehead et al., 2016) and at high altitudes (Gabey et al., 2013). The WIBS is a three channel LIF instrument developed by the University of Hertfordshire and manufactured by Droplet Measurement Technologies LLC available with different versions (e.g., WIBS 4A and WIBS NEO) of slightly different optical and electronic configuration (Gabey et al. 2010; Perring et al. 2015). In parallel with the measurement of fluorescent aerosol particles (FAP), the CCN and condensation nuclei (CN) number concentrations were also measured in order to determine what fraction of the total particle population was composed of CCN and FAPs.

The primary objectives of this exploratory study are to evaluate the physical properties of CN, CCN and FAP, investigate correlations between CCN and FAP, analyze trends related to

meteorological factors, and compare the FAP measurements with those from previous studies that documented fungal and pollen spores using off-line analyses.

2 Measurement and analysis methodology

2.1 Measurement site and experimental setup

The measurement site (Fig. 1a) is the Facundo Bueso (FB) building on the University of Puerto Rico, Rio Piedras (UPR-RP) Campus (18°24'6.4"N, 66°03'6.5"W, 6 m a.m.s.l.), and for the airborne spores were collected using the Hirst-type Burkard sampler (Burkard Scientific Ltd, Uxbridge, UK). located on the rooftop of the Medical Sciences Campus (MSC) of the University of Puerto Rico (18°23'48" N, 66°4'30" W, 60 m a.m.s.l) both located in San Juan, which is the urban capital of Puerto Rico (pop. 2,448,000). Moreover, the measurement sites are located at the center of the San Juan city (199 km^2), a clear representative of typical urban atmosphere. San Juan has a tropical climate, receiving a significant amount of rainfall (4.22±1.3 in) throughout the year. The FB site is surrounded by various sources of emission such as residential cooking, roadway traffic, and vegetation. Because of the urban location, aerosol emissions from roadway traffic and nearby residences contribute significantly to the total aerosol number concentrations at the site.

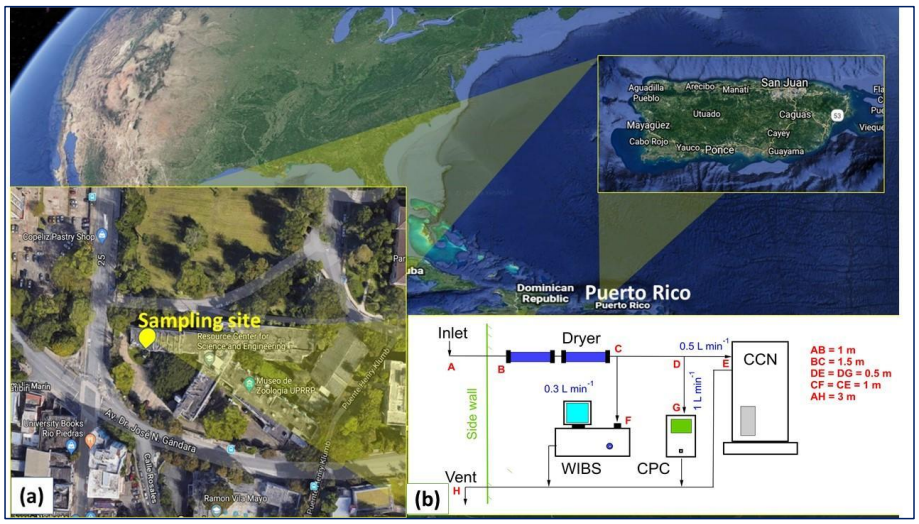

Figure 1. (a) Sampling location in the FB building of UPR-RP (b) experimental setup comprising the cloud condensation nuclei counter (CCN), condensation particle counter (CPC), and the wideband integrated bioaerosol sensor (WIBS). This figure was generated using © Google Earth Pro 7.3.

Sampling was performed for eight consecutive days (September 16-23, 2019). The measurement setup consisted of two diffusion dryers (TSI model 3062) connected in series, a cloud condensation nuclei counter (CCN-100, Droplet Measurement Technologies), a condensation particle counter (CPC, TSI model 3772), and a wideband integrated bioaerosol sensor (WIBS-NEO, Droplet Measurement Technologies) (Fig. 1b). Atmospheric aerosol samples were aspirated from the exterior through the sidewall of the laboratory (~3 m above the ground) with conductive tubing (1/4" internal diameter and 1 m length). The aerosols were dried as they passed through two diffusion dryers (< 10% RH) containing silica gel and then continued on to a manifold connected to the WIBS, CCN100, and CPC which sampled at flow rates of 0.3, 0.5, and 1 L min^{-1}, respectively. Particle losses due to sedimentation, diffusion, and inertial separation along the sampling lines were calculated for each of the instruments (Kulkarni et al., 2011). The particle sampling efficiency with respect to particle size is shown in the Supplement (Fig. S1). The sampling efficiency calculated for the particle size range 0.1-3 µm is greater than 80 %. However, the sampling efficiency is reduced greatly for particle sizes above 3 µm. The experimental setup allows WIBS NEO to receive particles up to 6 µm with more than 60% efficiency. Due to calculation uncertainties, we have chosen not to correct the data for these estimated losses because we are interested in the relative changes in the size distributions with respect to time and meteorology. The WIBS NEO, like all single particle, optical spectrometers, measures what is designated an "equivalent optical diameter (EOD)" that is defined as the size of a particle scattering the equivalent intensity of light as a spherical particle with known refractive index. Given that bioaerosols, dust and other types of environmental aerosols are not spherical, and their refractive index is unknown, the geometric size can be estimate to, at best, ±20%, hence relative size is more relevant than absolute size. Therefore ~~T~~the absolute size of the particles is not a factor in our current analysis.

2.2 Instrumentation

The CCN-100 used in this study is a continuous-flow, thermal-gradient, diffusion chamber that measures the concentration of aerosols activated as cloud droplets as a function of supersaturation (SS). Aerosol samples are drawn into a 50 cm tall column (inner diameter 2.3 cm) whose inner walls are saturated with water. A series of heaters along the column are controlled to maintain a temperature gradient from cooler to warmer as the particles move down the column. Since water vapor from the wetted column diffuses to the particles faster than the heat, a supersaturated condition is maintained that is determined by the temperature gradient and flow rate~~A series of heaters are controlled to maintain a temperature gradient from cooler to warmer as the particles move down the chamber. The difference in diffusion rates between heat and water vapor creates a supersaturated environment at the centerline of the cylinder~~. Those aerosol particles that can activate as a cloud droplet at the constant SS in the chamber will begin growing as water molecules diffuse to the particle surface and at the downstream of the column, an optical particle counter measures the number size distribution of the cloud droplets within the size range of 0.75–10 µm. For more an in-depth description of

Formatted: Normal (Web), Space Before: 1.5 pt, After: 1.5 pt, Line spacing: single

Formatted: Font: 12 pt, Not Bold

Formatted: Font: 12 pt

Formatted: Font: (Default) Times New Roman, 12 pt

the operating principle and calibration procedures the reader is directed to the paper by Roberts and Nenes (2005). In our study, the supersaturation (SS) was maintained at 0.3%, a SS that is in the range of what would be encountered in convective clouds similar to those that form over the island of Puerto Rico (Duan et al., 2012: Uin et al., 2016).

To measure the total concentration of environmental particles > 0.01 μm we used a butanol-based, condensation particle counter (CPC, model 3772 TSI) where the aerosol sample is drawn continuously through a heated saturator in which butanol vapor diffuses into the aerosol stream. An external vacuum pump was used to draw the aerosol samples at 1 L min^{-1}. This CPC employs a single particle count mode to measure the particle number concentrations up to 10^7 L^{-1} at an accuracy ±10%. The detailed design and working principle of the CPC are described by Stolzenburg and McMurry (1991).

The WIBS measures the fluorescent characteristics of aerosols using ultraviolet, light-induced fluorescence (UV-LIF) (Kaye et al., 2005; Stanley et al., 2011). This instrument provides detailed information on fluorescing bioaerosols on a single particle basis. The detection principles of the WIBS are discussed elsewhere (Kaye et al., 2005) and briefly described here. Atmospheric particles are drawn into the WIBS via a laminar flow delivery system and pass through the path of a continuous-wave diode laser (635 nm), which acts as a source for particle sizing and shape detection. The total flow is approximately 2.4 L min^{-1} of which 2.1 L min^{-1} is introduced in the form of sheath flow (i.e., filtered air) and 0.3 L min^{-1} is sample flow to maintain the particle alignment with the 635 nm laser. The forward scattering of the light is detected by a quadrant photomultiplier tube (PMT) and is used to determine the asphericity factor (AF) of the particles which roughly estimates the shape of the particles (Gabey et al., 2010). Experimental evidence shows that the AF is near zero for a perfectly spherical particle, while it approaches 100 for a fiber or rod-like aerosol particle (Kaye et al., 2007; Gabey et al., 2010). The light scattered from the diode laser is used to activate, sequentially, two Xenon lamps that are filtered to illuminate the particles with UV light at 280 nm and 370 nm, respectively. The wavelengths were specifically selected to excite fluorescence in particles containing tryptophan (280 nm) and nicotinamide adenine dinucleotide (NADH, 370 nm). There could be numerous molecules that can be excited by fluorescent light. For examples molecules such as proteins, vitamins, large polymers, molecules having conjugated double bonds, heterocyclic aromatic compounds, particularly when nitrogenous substituents are present. Tryptophan is an amino acid that has the highest (~ 90%) fluorescence in the native protein. Nicotinamide Adenine Dinucleotide Phosphate (NAPDH) is one of the major

contributors to the fluorescence signal when attached to the protein molecule and is produced widely in the metabolic cell. The fluorescence from the 280 and 370 nm excitations is recorded by PMT detectors, one that is filtered for 310-400 nm emissions and the other for 420-650 nm. Hence, when a particle is excited at either of the incident wavelengths, there are four possible responses: 1) no fluorescence is detected, 2) when excited at 280 nm the particle fluoresces at a wavelength in the 310-400 nm waveband (FL1), 3) when excited at 280 nm the particle fluoresces at a wavelength in the 420-650 nm waveband (FL2), or 4) when excited at 370 nm the particle fluoresces at a wavelength in the 420-650 nm waveband (FL3). The fluorescence characteristics of an individual particle are determined in any of the three fluorescence channels when its fluorescence emission intensity exceeds a baseline threshold. The baseline threshold is determined using the approach by Perring et al. (2015) that incorporates the daily data sets to remove background artifacts. Particles that exhibit fluorescence lower than the baseline threshold were treated as non-fluorescent particles. A particle that fluoresces when excited by either of the xenon lamps may also produce emissions in both the 310-400 and 420-650 wavelength; hence, from the FL1, FL2 and FL3 signals there are seven possible combinations, generally accepted by the WIBS community, that have been designated fluorescence types A, B, C, AB, AC, BC, and ABC (Perring et al., 2015). Types A, B and C refer to particles that fluoresce only in FL1, FL2 and FL3. The other four types are the respective combinations of the A, B, and C.

It should be noted that A and C channels are highly sensitive to fluorescent bioaerosol particles whereas the B channel is cross sensitive to non-biological aerosols (Gabey, 2011). Using the fluorescence data for single particles from these three individual channels, the FAP can be characterized and discriminated from non-biological aerosol particles. Based on the above description, the WIBS records the optical size, particle asphericity factor (AF), fluorescent excitation-emission matrix and the total number concentration (N_{WIBS}), which includes non-fluorescing, and total FAP on single particle mode collected within the size range from 0.5 to 30 µm. Before deployment, the WIBS was factory calibrated for the size, sphericity and fluorescence using reference fluorescent polystyrene latex spheres which are traceable to National Institute of Standards and Technology (NIST).

Note, it is important to emphasize that although the WIBS was designed to detect fluorescence from biological particles, it is unable to unequivocally differentiate what type of bioaerosol fluoresced, e.g., if the particle was bacteria, fungus, or pollen. There are a number of studies, such as those by Hernandez et al. (2016), that have used the WIBS in laboratory studies to

characterize a variety of species of bacteria, fungi, and pollen. Such studies have shown that these three types of bioaerosols fall in general categories of size and fluorescence type. These categories will be discussed further on in this paper in the context of comparing the FAP characteristics in San Juan to those reported in controlled laboratory experiments.

The CPC measurements, taken at 1 Hz, are averaged to five minutes intervals for comparison with the WIBS and CCN measurements that are also averaged in five-minute intervals. In addition, the particle by particle (PbP) data from the WIBS are used to create size distributions and analyze fluorescence properties and interrelationships in greater detail.

2.3. Fungal spore data

The fungal spore data were obtained from the department of Microbiology of the Medical Sciences Campus of the University of Puerto Rico. The enumeration of outdoor spores used the 12-traverse methodology proposed by the British Aerobiology Federation (Caulton and Lacey, 1995). Airborne spores were collected using a volumetric Hirst-type sampler, specifically a Burkard (Burkard Scientific Ltd, Uxbridge, UK). This equipment was located on the rooftop of the Medical Sciences Campus of the University of Puerto Rico, 30 meters above ground level. The Burkard 24-hr trapping system worked continuously with an intake of 10 ~~liters of air/min~~L min^{-1}. Fungal spores were impacted on a microscopic slide coated with a thin layer of 2% silicon grease as a trapping surface. The slide was changed daily and mounted on polyvinyl alcohol (PVA) mounting media for microscopic examination. Counting was done on each preparation along 12 traverse fields every 2 hours for a total of 12 hours on the longitudinal traverse. Spores were identified based on their morphological differences (Quintero et al. 2010). The identification was performed by means of a bright-field optical microscope NIKON Eclipse 80i microscope (Nikon Manufacturing), using a magnification of 1000X.

Formatted: Superscript

2.4. Meteorological data

Hourly meteorological data e.g., temperature (℃), relative humidity (RH, %), wind speed (WS, m/s) and wind direction (Degree) were provided by the department of natural science taken from a weather station that is located around ~800 m away from the aerosol instrumentation.

2.5. Air mass back trajectories

Twenty-four-hour air mass back trajectories, ending at 100 m above mean sea level, were obtained from the Hybrid Single Particle Lagrangian Integrated Trajectory Model (GDAS, 1-degree resolution, HYSPLIT) to identify the possible source of the aerosols.

3 Results and Discussion

3.1 Time series of the particle number concentrations

Figure 2a shows the temporal pattern of particle number concentrations of CN, CCN (at 0.3% SS) and N_{WIBS} (0.5 - 30 µm) averaged in 10-minute intervals. The average particle number concentration measured by the CPC was (3±1)×10^6 L^{-1}. This value is higher than the CN number concentrations reported previously at other more remote locations on the island, such as at the northeast coastal site of the Cabezas de San Juan nature reserve and at the Pico del Este, in El Yunque National Forest, where the CN concentrations were (9±5)×10^5 and (11.6±3)×10^5 L^{-1}, respectively, both as reported by Allan et al. (2008). The differences in CN concentrations are related to the geographical locations and average climatic conditions of the other regions discussed. The measurement site (Facundo Bueso) is an urban location influenced by emissions from vehicular traffic, vegetation, and other human activities such as heating and cooking. The Cabezas de San Juan is a remote coastal location where the atmosphere is relatively clean, influenced by marine aerosols or long-range transported aerosols. The Pico del Este is a mountainous region that has a significant influence of aerosol from the nearby vegetation and from particles transported from marine boundary layer. The CN concentrations show systematic, daily trends that reflect the emissions from motorized vehicle traffic and nearby residential heating and cooking. ~~The CN concentrations show systematic, daily trends that reflect the motorized vehicle traffic and nearby residential emissions, the latter mostly from cooking~~. The mean CCN concentration of (1.5±0.5)×10^5 L^{-1} is about 20 times lower than the CN, i.e. only about 5% of the measured aerosol particles would activate as cloud droplets at a SS of 0.3%. This implies that particles over the site are mostly non-hygroscopic or of low hygroscopicity.

The number concentrations of N_{WIBS} and FAP were (7.3±5)×10^4 and (5±3)×10^3 L^{-1}, respectively, which are approximately 40 and 600 times lower than the CN concentrations. Given the differences in the lower size thresholds for the CPC and WIBS with respect to the smallest detectable particle, 10 nm for the CPC and 500 nm for the WIBS, this implies that about 98% of the particles are smaller than 500 nm. The FAP concentrations showed a

Formatted: Font: (Default) Times New Roman, 12 pt

Formatted: Font: (Default) Times New Roman, 12 pt

Formatted: Font: (Default) Times New Roman, 12 pt

Formatted: Font: (Default) Times New Roman, 12 pt

342 systematic daily cycle where nighttime particle concentrations were relatively higher than
343 during the daytime, this is being driven primarily by the type ABC FAPs as illustrated in Fig.
344 2b where the type ABC concentrations are mostly much higher than other types. The types AB
345 and AC concentrations have trends similar to the type ABC.

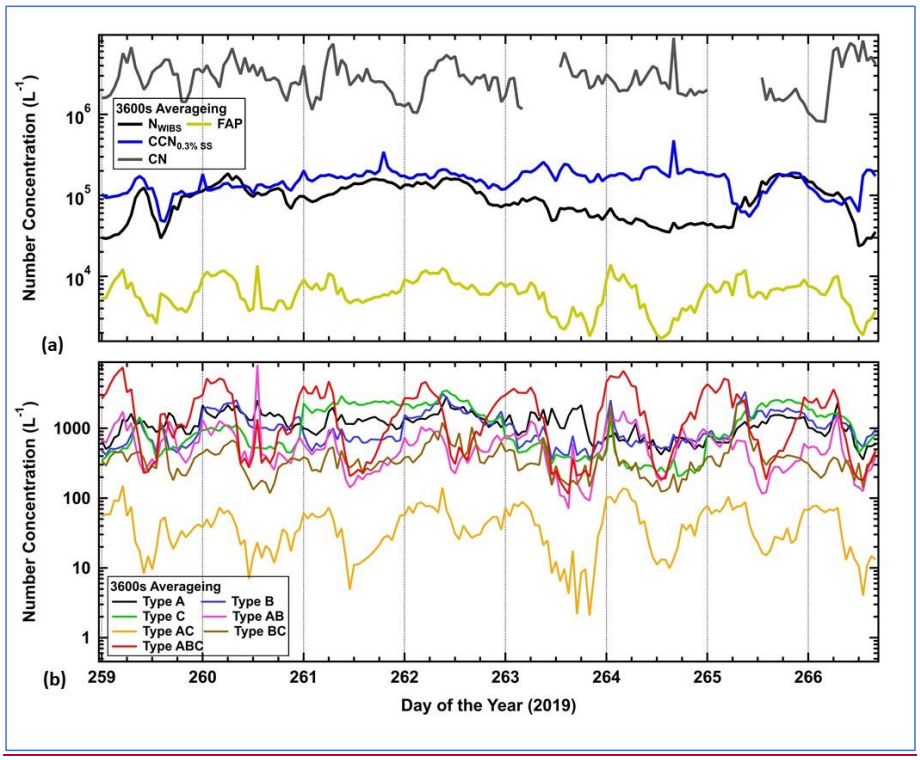
3600s Averageing
N_WIBS
FAP
CCN0.3% SS
CN
Number Concentration (L-1)
(a)
3600s Averageing
Type A
Type B
Type C
Type AB
Type AC
Type BC
Type ABC
Number Concentration (L-1)
(b)
Day of the Year (2019)

346

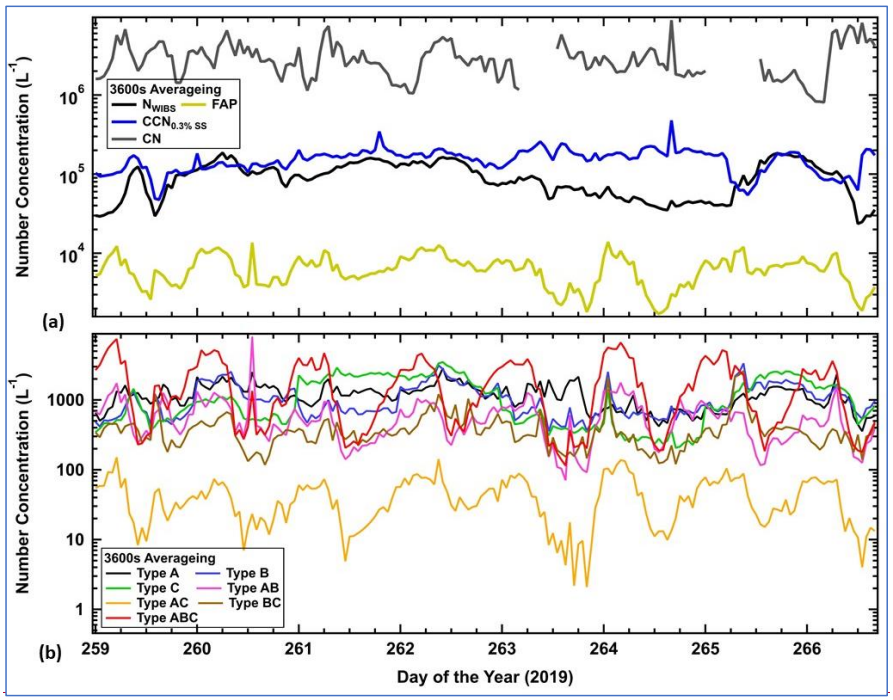

Figure 2. Time series of the number concentrations. (a) CN, CCN, N_{WIBS} and FAP. (b) FAP types A, B, C, AB, AC, BC, and ABC. The gaps in time of the CN concentrations were when the CPC was offline.

In the time series of number concentrations in Fig. 2 there are what appear to be periodicities in the CN, CCN and FAP. This periodicity is seen more clearly in the concentrations averaged by the time of the day (over the whole measurement period) as shown in Figs. 3a and 3b. Figure 3a highlights the diel trend in CN concentration (black curve) that begins increasing at 4 am, reaches an initial peak at 7 am, is followed by a second peak four hours later at 11 am then begins decreasing the remainder of the day. The CCN measurements show a trend of increasing concentrations early in the morning but does not start its rapid increase until midday peak, then it begins increasing until reaching its peak around 4 pm, five hours after the CN peak. Prior to the afternoon peak, there are smaller peaks that occur at 2 am and 8 am~~The CCN concentration shows an increasing trend early in the morning but doesn't start its rapid increase until midday when it begins increasing until reaching its peak around 4 pm, five hours after the peak in the CN~~. The N_{WIBS} and FAP concentrations are drawn in magenta and green, respectively. The N_{WIBS} shows an increase in the morning with an initial peak at 7 am, similar to the CN;

Formatted: Font: (Default) Times New Roman, 12 pt

however, these concentrations then decrease until peaking again in the late afternoon, an hour after the CCN peak. The average FAP concentrations remain elevated between midnight and 6 am, after which they decrease by about 30% and remain fairly constant the remainder of the day.

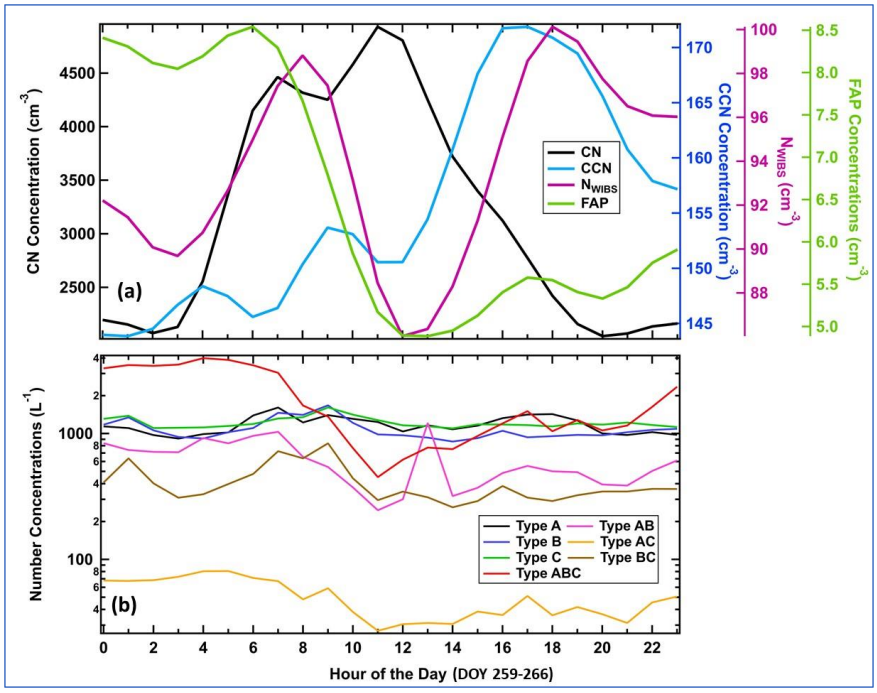

Figure 3. (a) Hourly concentrations of CN (black curve) and CCN at 0.3% supersaturation (solid blue curve), N_{WIBS} (magenta) and FAP (green) concentrations. (b) Hourly concentrations of the seven types of FAP.

Figure 3b displays the hourly behavior over the averaged, 24-hour period of the seven types of FAP. For all of the types except the AC and ABC, the FAPs remain relatively constant throughout the day. The types AC and ABC are elevated in concentration between midnight and around 6 am, both about a factor of three higher during those hours than during the remainder of the day. Although the types AC and ABC follow the same trend, the type ABC is about 50 times larger and dominates the FAPs during those hours. During the remainder of the day, the types A, B and C are approximately equal in concentration.

3.2 Temporal trends of the particle size distribution

Figure 4 shows the size distributions of total (Fig. 4a) and FAP (Fig. 4b) number concentrations measured from September 16 to September 23, averaged in 10-minute intervals. The color scale is the log of the concentration. The white curves are the average median volume diameters for the total (Fig. 4a) and FAP (Fig. 4b). The total number size distributions show an irregular trend of increasing concentrations over all sizes, usually occurring around midday on all days except on the day of the year (DOY) 264 when the size distributions remain approximately the same throughout the day. In contrast, the FAP size distributions have a more regular, daily pattern whereby the concentrations increase over all sizes to a maximum between midnight and 6 am.

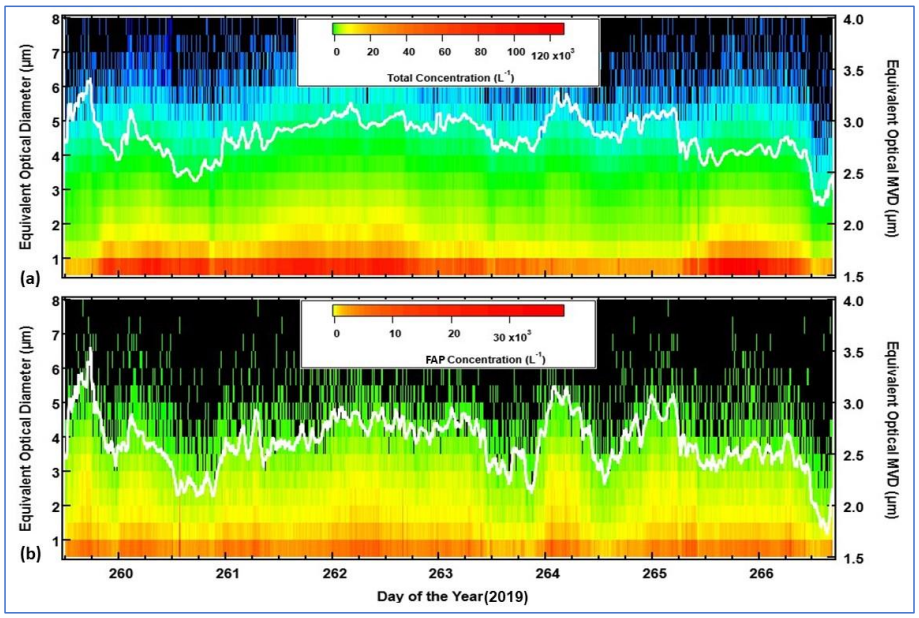

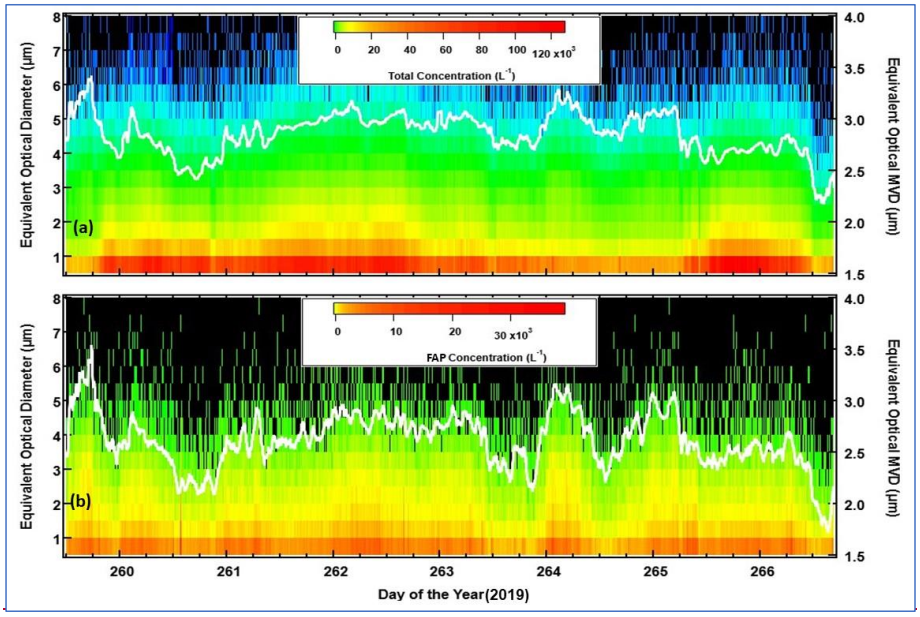

Figure 4. Time series of total (a) and (b) fluorescent particle size distributions measured by WIBS for the period September 16-23 (DOY 259-266), 2019. The white curves are the average median volume diameters (MVD).

The daily trends of the size distributions of the seven different types of fluorescent particles are shown in the Supplement (Fig. S2). where we observe that ABC and AB types were dominant at the site with a unique and systematic diel cycle. Reflecting the behavior of the total concentrations in Fig. 3b, the average EODs of ABC and AB type particles increase at night when the particle size grows to >4 μm by midnight. Fluorescent type A does not show any specific temporal trend while types B and C have periods when the concentrations increase over all sizes but do not follow the trends of the ABC and AB types particles. The type BC and AC particle concentrations are much lower than the other types.

The increases in the modal diameter from daytime to nighttime, seen in the Supplement (Fig. S2), particularly for the types AB, AC and ABC, was further investigated by comparing the size distributions averaged at night and in the daytime. We have plotted the particle size distributions for these three FAP types (Fig. 5), averaging from noon to 6 pm (red shading) and from midnight to 6 am (blue shading) over the whole measurement period (DOY 259-266). These two periods represent time intervals when the number concentrations and average sizes exhibit the largest differences. All three FAP types show a shift towards larger sizes from daytime to nighttime; however, the type ABC particles have the most distinctive shifts (Fig. 5c), indicative of both a general increase in concentration over all sizes but a very clear, larger increase proportionately at EODs larger than 2 μm.

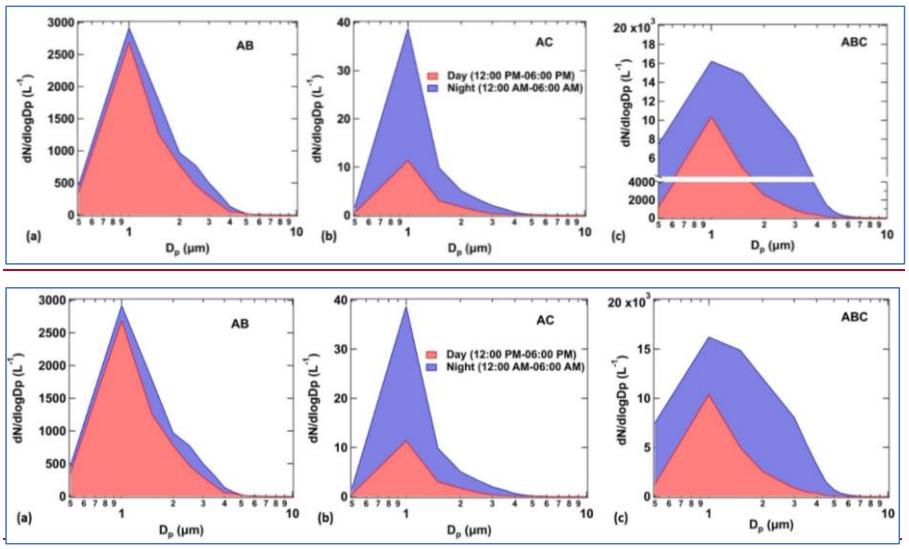

Figure 5. The size distributions from types (a) AB, (b) AC and (c) ABC were averaged from 12 pm to 6 pm (red shading) and from midnight to 6 am (blue shading) for the eight days of the project.

3.3 Asphericity

The asphericity derived from the quad detector of the WIBS is a relative indicator of the shape of each particle as shown in the supplement (Fig. S3) for FAP type (AB, AC, and ABC) and for all particles including the non-FAP. The color scale shows the average asphericity at each size interval over the duration of the project. Among the fluorescent types, the asphericity of ABC particles shows a mode between 2 and 4 µm during nighttime, especially at midnight. The asphericity size distributions of all particles show a broader mode of enhanced asphericity between 2 and 4 µm that varies somewhat but not in a noticeable diel pattern. Note that particles with asphericities < 20 are generally considered quasi-spherical so that the values that are shown here indicate slight changes in shape, on average, of type ABC particles, as well as all particles, but the overall population of particles can be considered quasi-spherical.

Asphericity of non-fluorescent (non-FAP) particles was always observed higher than the FAP (Fig. S3d in the Supplement). The higher values of asphericity of non-FAP particles can be seen between size 3 and 6 µm every day and dominate on DOY 261 and 262.

3.4 Air mass back trajectories

Air masses arriving at the site on DOY 259 and 264 were coming from the northeast of the island originating 24-hours earlier over the Atlantic Ocean. The air masses that arrived on DOY 260-63 and 266 were from the southeast of the island and on DOY 265 the air was from the south-southeast. Figure S4a shows that all of the air masses had been < 50 m above the surface the entire 24-hour period before arriving at the measurement site. The one exception was on DOY 259 when the air mass had stayed above 200 m from 12 to 24 hours then began descending as it approached the island. This same air mass was associated with rain formation close to the measurement site (Fig. S4b in the Supplement). The air mass on DOY 264 came across the islands to the SE of Puerto Rico (e.g., Culebra and the British Virgin Islands), possibly mixing the marine aerosols with polluted emissions before arriving at the measurement site. Likewise, the air mass trajectory on DOY 260 and 262 crossed over the Vieques and US Virgin Islands at a low altitude, likely mixing with anthropogenic emissions. The air mass arriving on DOY 261 is comparatively dry as no rainfall happened along its trajectory, but it also crossed over the Vieques island. The increment in total particle number concentrations on DOY 260-262 and DOY 266 shown in Fig 4a are possibly attributed to air mass arrived over the Islands in the Southeast of Puerto Rico. It could be the reason why we observed higher values of asphericity of non-FAP on DOY 261 and 262. The remainder of the air masses were presumably not impacted by anthropogenic emissions until arriving over the Puerto Rico landmass.

Formatted: Normal (Web)

3.5 Meteorological data

Figure S5 shows the temperature and relative humidity (RH) (Fig. S5a in the Supplement), and the wind speed, wind direction and precipitation (Fig. S5b in the Supplement). The average wind speed, temperature, and RH for the period of measurement were 2.8±2.4 m/s, 29±2 ℃, and 77±11 %, respectively. The DOYs 259 and 265 received significant rainfall of 1.35 and 1.84 inches, respectively. Note that these two days are also those that the back trajectory analysis indicated that rain had formed in the arriving air masses. The wind speed and direction, temperature, and RH show a systematic daily cycle where the wind speed and temperature peaked during midday (2.8±0.7 m/s and 33±1 ℃), and the RH peaked around midnight (91±3 %). Wind profiles at the measurement site show that the air was flowing from 135˚- 250˚during the night then from 93˚-134˚during the daytime. On DOY 262 and 265, as well as the afternoon of DOY 259, the winds are comparatively low. The average wind speeds at night (0.24±0.2

m/s) compared to those during the day (2.8±0.6 m/s) suggest generally calm wind conditions that are normal this time of year when not under the influence of tropical storms.

To further highlight the relationships between the meteorological conditions and FAP, we computed the hourly averages of RH, wind speed and FAP concentrations during each 24-hour period over the eight-day period and compared them in Fig. 6a. The RH and FAP concentrations are maximized during the hours from midnight to 6 am while wind speed is at a minimum during those hours, maximizing a little after midday.

The relationship between RH and the FAP fraction is further underscored in Fig. 6 where there appears to be an RH threshold below about 80% that the FAP fraction remains below 0.1 but then increases rapidly to greater than 0.3 as the RH exceeds 90%, i.e. less than 10% of the particles measured in the size range of the WIBS were FAP when the RH < 80%, but increases to more than 30% at high humidities. The increase of FAP D_{mvd} and the number concentrations depend on the hygroscopicity of the particles. Among the different FAPs measured at the site, the ABC, AB, and AC types were observed to have systematic diel patterns and were believed to be more hygroscopic than others. Therefore, the D_{mvd} and FAP number concentrations were increasing when RH reaches 80% and above. The other spread of points at >80% RH were possibly the less hygroscopic FAP types such as the A, B, C, and BC, not showing any increasing trend in D_{mvd} and the number concentrations. The difference between Fig. 6b and 6c are how the markers are color coded. In Fig. 6b, the coloring denotes the equivalent median volume diameters (D_{mvd}) and in Fig. 6c, the coloring is the FAP concentration. Both the D_{mvd}s and concentrations increase with increasing humidity and FAP fraction.

Formatted: Normal (Web)

Formatted: Subscript

Formatted: Subscript

Formatted: Subscript

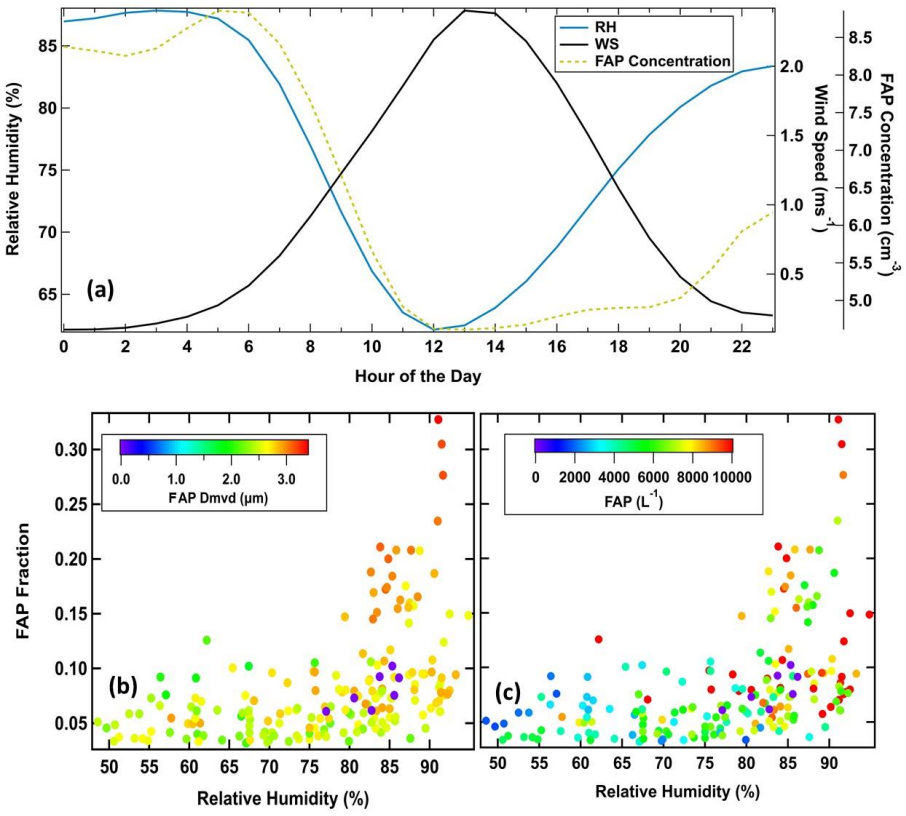
RH
WS
FAP Concentration
Relative Humidity (%)
Wind Speed (ms-1)
FAP Concentration (cm-3)
(a)
Hour of the Day
FAP Dmvd (μm)
FAP (L-1)
FAP Fraction
(b)
(c)
Relative Humidity (%)
Relative Humidity (%)

488

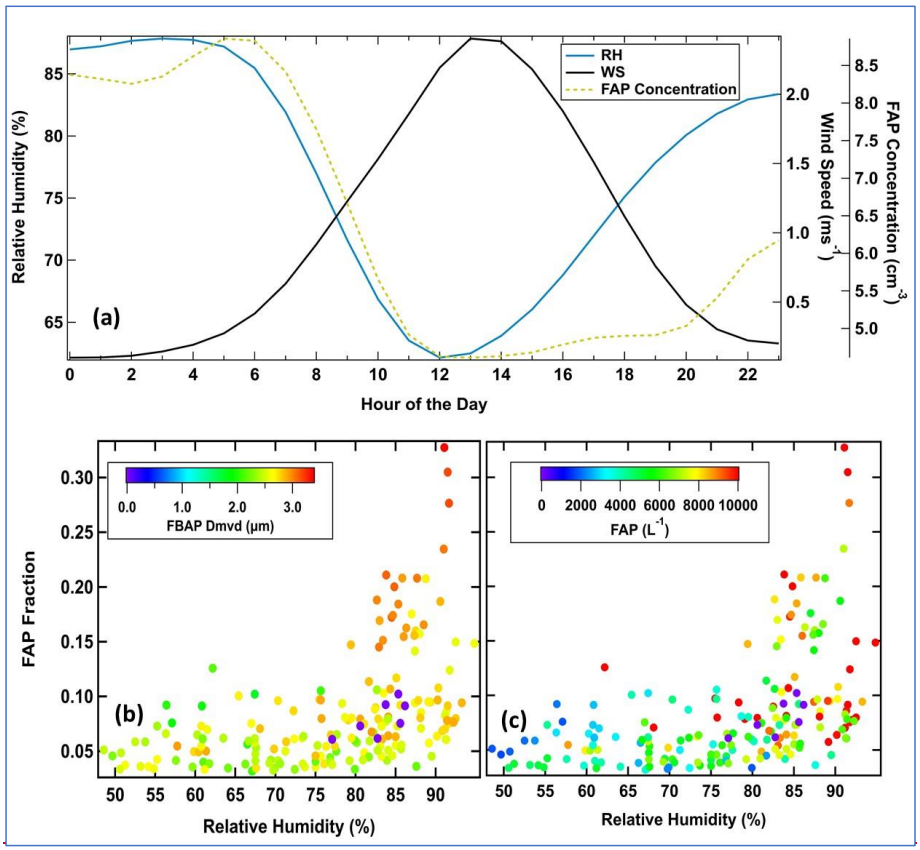

Figure 6. (a) hourly averages of relative humidity (blue curve), wind speed (black) and FAP concentration (green dotted). (b) link between fluorescent fraction and relative humidity (FAP particle volume weighted equivalent optical diameter. D_{mvd}, on the color scale). (c) fluorescent fraction and relative humidity (FAP particle concentration on the color scale). The data in all the figures averaged over DOY 259-266.

3.6. Fungal spore data

The time series of the fungal spores, measured on the rooftop of the medical science building at the university, are shown in Fig. 7. Similar to the FAP number concentration and fraction, the spore concentrations have a diel trend with maxima around midnight. The average concentrations were 48±42 L^{-1} with a maximum 112±44 L^{-1} around midnight. We calculated positive correlations of 0.7, 0.47, and 0.54 between the total spore concentration and concentrations of FAP types ABC, AB, and AC types, respectively. Previous studies for this

region reported the most common fungal genera detected were the Basidiospores and Ascospores (Quintero et al., 2010; Rivera-Mariani et al., 2011). Figure 7b illustrates the distributions of outdoor fungal spore types recorded at MSC of the University of Puerto Rico. Fungal species were identified and distributed different categories, referred to as hyphae or filamentous spores, macroconidia >10 µm, microconidia 3-10 µm, microconidia < 3 µm, and unidentified spores presented in others category. We observed that the microconidia 3-10 µm contributed the highest (81%) fraction to the total fungal species followed by microconidia (<3 µm) 3.86% and Macroconidia (>10 µm) 1.8%. We observed that the Basidiospores contributed the highest (49.4%) fraction to the total fungal spores type followed by Ascospores 19%, Diatrypaceae 8.6% and Penicillum/Aspergillus 3.86%. The mean concentrations of dominant species such as Basidiospores, Ascospores, Diatrypaceae and, Penicillum/Aspergillus were 24±20, 9.3±4, 4±3 and 2±1 L^{-1} during the study period. The Ascospores and Penicillum/Aspergillus had more elevated concentrations during the night while Diatrypaceae concentrations were generally higher during the daylight hours.

These species were the most common airborne spores in San Juan, present throughout the year and predominated during September (the rainy month). The WIBS's ABC and AB types were likely the Basidiospores and Ascospores (Fig. 7b). Previous studies (Quintero et al., 2010; Rivera-Mariani et al., 2020) reported that the most common fungal genera detected were the Basidiospores and Ascospores in the San Juan atmosphere. Which is also confirmed in this study. The size of the Basidiospores and Ascospores (10-20 um) is usually larger than Aspergillus, Penicillium, and Cladosporium spores. Furthermore, we observed a systematic diel pattern in the number concentrations of these fungal spores which is strongly correlated to diel pattern of FAPs detected in ABC channel of WIBS. The other genera most frequently detected were the Penicillium/Aspergillus, Cladosporium and Ganoderma, present at low concentrations reported by Quintero et al. (2010). Those species possibly corresponded to WIBS's AC types which were systematic and relatively low concentrations. These fungal spores, present between the midnight and early morning period, suggest an active release mechanism induced by the morning hours dew point and increased humidity under calm wind conditions, in concordance with the findings reported by Quintero et al. (2010).

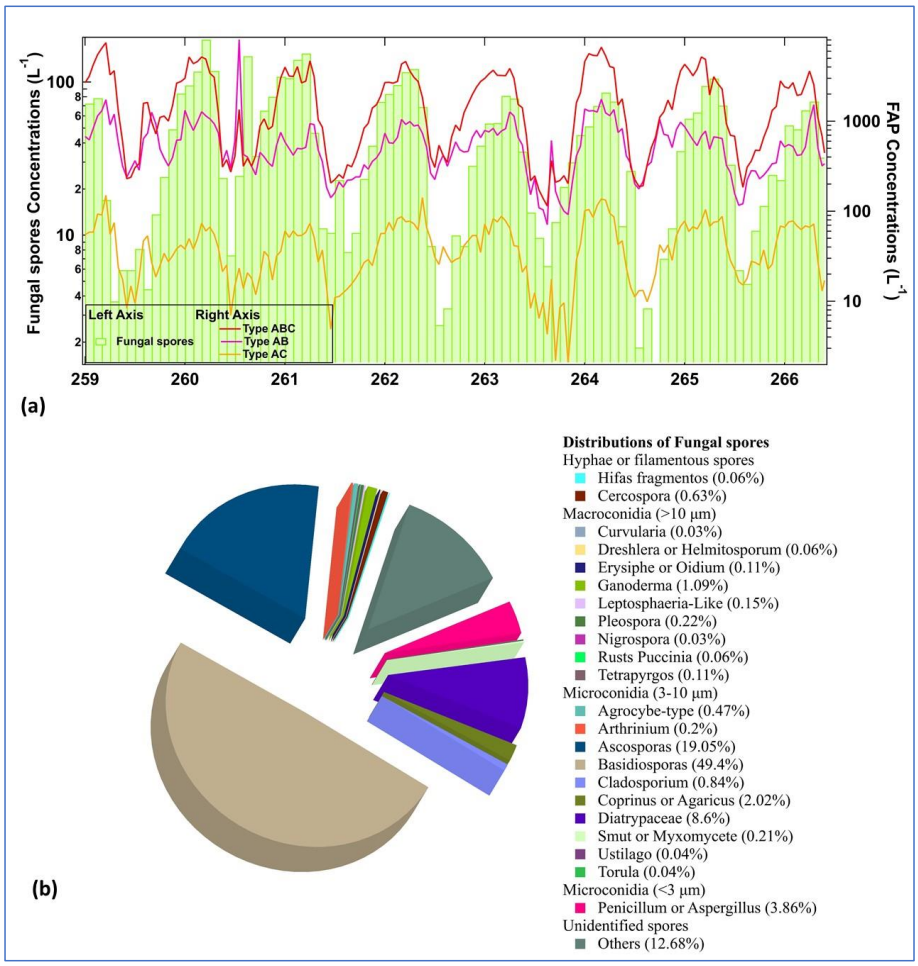

Figure 7. (a) time series particle number concentrations of fungal spores (left axis) measured at the Medical science department and the FAP types ABC, AB and AC (right axis) detected by WIBS at FB site. (b) distributions of outdoor fungal spores recorded at Medical Sciences Campus, San Juan.

4. Discussion

From the results presented above, the following features stand out: 1) The CN, CCN and FAP concentrations have daily patterns during which each maximizes at a different hour of the day, 2) the periodic FAP concentration is predominantly of the type ABC that reaches a daily maximum around midnight and the asphericity of this type of FAP increases slightly during

the same time period, 3) the RH reaches a maximum each day around midnight, 4) the wind speeds are a minimum around midnight and 5) an independent analysis of bioaerosols using fluorescence microscopy to identify spore types revealed a periodicity of spore concentrations that was highly correlated with the RH and FAP type ABC concentrations.

Referring back to Fig. 3a, the CN, CCN, $N_{WIBS,}$ and FAP concentrations all exhibit a diel periodicity but with peak values occurring at differing hours. The CN population encompasses all environmental particles larger than about 10 nm and are dominated by anthropogenic aerosols, i.e., those produced from residential cooking and local vehicular traffic. Given that the WIBS measures the concentration of particles larger than 0.5µm, and that the total concentration has an average peak maximum of 100 cm^{-3}, compared to a maximum CN concentration 5000 cm^{-3}, this implies that 98% of the particles have sizes smaller than 0.5µm. The rest are the coarse mode aerosol (2%) is typically smaller in number concentrations, yet high in mass ~~A~~concentrations. A comparison of the maximum CCN and N_{WIBS} concentrations, 170 cm^{-3} vs 100 cm^{-3}, leads us to conclude that most of the CCN are in sizes greater than 0.5µm. Likewise, since the maximum CCN concentrations are only about 2% of the CN values, this suggests that most of the CN have low hygroscopicity, a characteristic of fresh combustion particles.

The trends in the CN concentrations suggest that there are early morning activities that are producing emissions of anthropogenic particles. The two peaks are a result of the combination of two traffic patterns: the general city traffic as workers commute to jobs that are not on the university campus and vehicular traffic of university workers whose starting hours are later than the city workers. In Fig. 1a, the sampling site is located near the intersection of two major streets that carry both types of traffic. Unlike many large urban areas where morning and evening rush hour traffic can be distinctly seen in the CN measurements, there is a smaller density of cars during the evening commute than in the morning in San Juan.

The correspondence between the times of the two N_{WIBS} maxima and the CN and CCN peaks suggests that the > 0.5µm particles measured with the WIBS in the morning are a different mixture of compositions than the particles in the afternoon. The morning N_{WIBS} peak lags the first CN peak by an hour, likely as result of the primary emissions producing particles that grow into the size range of the WIBS; however, with the sunrise at around 6 am, temperatures begin increasing and the material in the more volatile particles begin to evaporate until the particle sizes decrease below the threshold of the WIBS. Some dilution will be occurring as the

boundary layer deepens with increasing temperatures, but this is a secondary effect as we do not see the CN concentrations decrease with the decrease in N_{WIBS}. Since the CCN concentrations remain low during this period, this implies that either the particles did not grow large enough to be good CCN or their composition is non-conducive for forming CCN. In the early afternoon we observe the CCN concentrations beginning to increase until reaching their late afternoon peak. The N_{WIBS} follows a very similar trend but lagged with respect to the CCN by a couple of hours. This afternoon trend in CCN has been identified in other large, polluted urban areas as the result of photochemical reactions producing hygroscopic, secondary organic aerosols (SOA) from photochemical reactions (Baumgardner et al., 2004). The N_{WIBS} is offset a couple of hours due to the time needed for the SOA particles to grow by condensation and aggregation. Finally, the FAP concentrations only begin increasing late in the evening after the CCN has maximized and their concentrations are less than 10% of the CCN. This suggests that if FAP are good CCN, they do not contribute significantly to the overall CCN population. It is important to note that contributions to the overall CCN populations depend on size, chemical composition, and number concentrations of particles.

Quintero et al. (2010) concluded that the release of the fungal spores that they measured and speciated was triggered by high RH and were found in multiple locations. Pollen spores, on the other hand, could not be linked conclusively to any meteorological factor. It is evident that almost all of the fungal spores are released in the El Yunque rain forest (Lewis et al., 2019). Two of the air sampling sites, Pico Del Este (PDE) and Cabezas de San Juan (CSJ) are very similar and very low in the fungal spores (less 5,000 spores/m^3). At another sampling site in El Verde (located to the west within El Yunque National Forest), the concentrations increase to 72,000 spores/m^3 and are found to have a decreasing gradient of fungal spores towards the Metro Area. For the rest of Puerto Rico, the Central Mountain Range is the other source of fungal spores. Bioaerosols, especially fungal spores, are very good ice nucleating particles (INP) (Kunert et al., 2019); however, except for periods with tropical storms, cloud tops rarely grow higher than the freezing level. On the other hand, these airborne spores may have the allergenic potential and could pose a health threat to sensitized population (references therein Quintero et al., 2010). Information about the presence and abundance of these spores will assist in the diagnosis of respiratory and allergic illness in Puerto Rico. Hence, given these previous results in comparison with the correlations that we have observed in the current study (Figs. 6 and 7), the type ABC fluorescing particles are most clearly linked to Basidiospores and Ascospores, the two species that made up the largest fraction of fungi measured with the

fluorescence microscopy. The hourly averages in Fig. 3b also showed that the type ABC only was predominant during the same period as the Basidiospores and Ascospores but then the other fluorescence types A, B and C were equally present during the remainder of the day. This is mirrored by the spore types shown in Fig. 7 that change in relative mixture during the day. Hence, by observing the relative changes in the seven FAP types, we get a qualitative measure of the changing population of bioaerosols.

Formatted: Font:

The WIBS characterizes the fluorescent aerosol particles using two-wavelength excitations and two-wavelength emissions. The sensitivity of types A and B to the intensity of the emissions in the 310-400 and 420-650 nm wavelength bands, when excited at 280 nm, in comparison to the intensity of emissions at 420-650 nm when excited at 370 nm has been exploited in the study by Ziemba et al. (2016) to identify differences in bioaerosol types as they relate to differences in FAP sources. In their study they were able to show a clear grouping of FAPs linked to source regions by plotting the ratio of type A to type B (emission sensitive) versus the ratios of type C to type B (excitation sensitive). We have followed a similar scheme; however, whereas the Ziemba et al (2016) study used a WIBS on an airborne platform flying over various land usage types, our site was fixed so we compute these ratios as a function of time rather than location. Figure 8 illustrates the periodicity of the type C to B ratio, increasing during those time periods that the type ABC concentrations were also increasing. Just as the sizes of FAP were seen to increase during these periods (Fig. 5), indicative of a change in FAP type, the shift in the type C/type B reflects the differences in the fungal spore types.

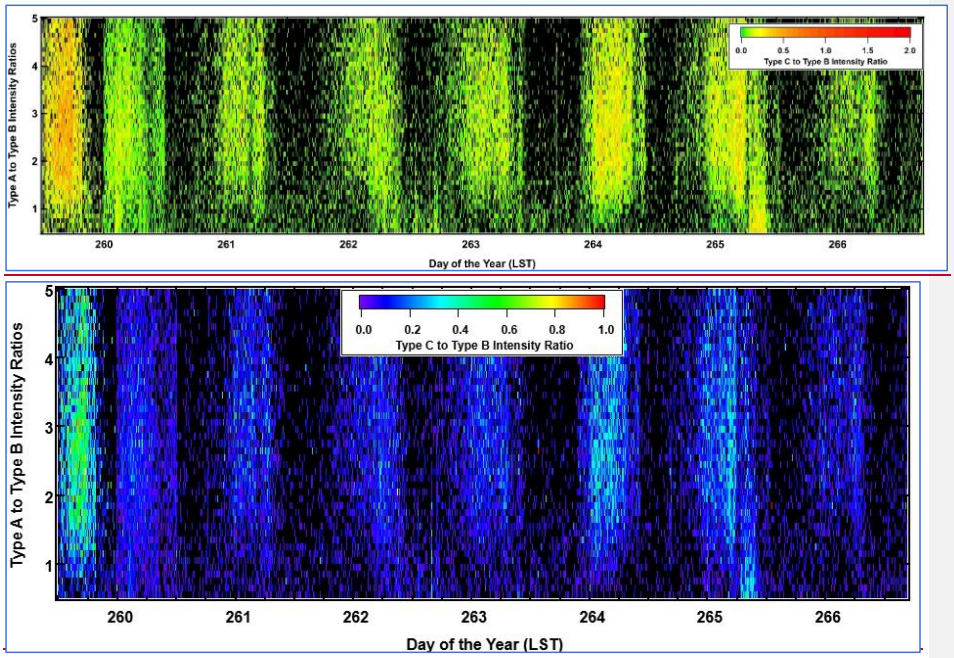

626

627

628 **Figure 8: Temporal distribution of emissions wavelength dependence (Type A to Type B) vs excitation**
629 **wavelength dependence (Type C to Type B).**

630

631 Hence, the changes in size distribution, asphericity, type C/B ratios, and speciated spore
632 concentrations, all occurring during the same time of day, provide independent verification that
633 a different type of PBAP is being produced during the periods of high RH than during the other
634 periods of the day.

635 The strong correlation between spore release and RH that has been highlighted in this study
636 has been previously reported, e.g., (Oliveira et al., 2005; Chi and Li, 2007; Gabey et al., 2013;
637 Calvo et al., 2018, Toprak and Schnaiter, 2013; Healy et al., 2014). None of those studies,
638 however, were from tropical regions nor they include the asphericity and FAP type rationing
639 to quantify their results.

640 Some laboratory studies have been conducted to measure the fluorescence characteristics of a
641 small variety of bacteria, fungi, and pollen, for example Hernandez et al. (2016) determined
642 that bacteria, fungi and pollen could be generally grouped according to the size and FAP type.
643 In their study, very few fungal spores were of the FAP type ABC such as found in the current

study. Instead, the majority of their fungi were types A and AB while the majority of type ABC spores were pollen, not fungi. On the other hand, the Hernandez et al. (2016) study did not test any of the major fungi species that were measured in the natural environment of Puerto Rico, i.e. Basidiospores and Ascospores.

5. Summary and Conclusions

A pilot study was conducted to evaluate the fluorescence and cloud condensation nuclei (CCN) properties of urban aerosols in San Juan, Puerto Rico, the first time such measurements have been made in this tropical city. Previous CCN measurements have been made on this island at coastal and rainforest sites, but no research has been pursued to see if bioaerosols are directly linked to CCN. There have been a number of laboratory studies conducted by other researchers who evaluated the CCN activity of various bacteria, fungi and pollen. Although some types of bioaerosols were found to be potential CCN, many others were not. Hence, the importance of bioaerosols as cloud forming particles remains an open question. The very large concentrations of fungal spores produced by flora in Puerto Rico, as reported by Quintero et al. (2010), along with the results from our pilot study, provided the initial motivation for the study reported here to assess if bioaerosols might contribute to the frequent cloud formation over the island.

The measurements were made from the Facundo Bueso building within the University of Puerto Rico, Rio Piedras Campus, from September 16-23, 2019, an urban location that experiences emissions from local residential cooking, vehicular traffic and a wide variety of flora. The site is located close to the intersection of two major streets carrying local business as well as university traffic.

In the pilot experiment, the CCN concentrations were measured with a commercial CCN spectrometer set at 0.3% supersaturation and the fluorescent properties were also measured with a commercial instrument, the Wideband Integrated Bioaerosol Spectrometer (WIBS). It is important to note that bioaerosols are not the only type of aerosol particle that will autofluoresce when excited at the wavelengths used in the WIBS, although care was taken to minimize interference from non-biological particles. Therefore, what is reported in the current study are the properties of fluorescing aerosol particles (FAP) without specifically labeling them as biological. In addition to measurements of CCN and FAP, the total concentration of condensation nuclei (CN) was documented with a condensation particle counter.

675 The mean number concentration measured by the CCN counter at 0.3% SS was (1.5 ± 0.5)
676 $\times 10^5$ L^{-1}, which was about a factor 21 lower than the average CN concentration $(3 \pm 1) \times 10^6$ L^{-1}. The mean FAP concentration was $(5 \pm 3) \times 10^3$ L^{-1}, which was a small fraction (~7%) of total
678 aerosol particle number concentration, N_{WIBS}, measured by the WIBS, whose lower size
679 threshold is 0.5 µm.

680 The CN, CCN, $N_{WIBS,}$ and FAP concentrations all have diel trends but their maxima occur at
681 varying hours of the day. The CN peaks at 6 am and 11 am due to business traffic and university
682 traffic that have different rush hours. The CCN reaches its maximum value at 4 pm as
683 photochemical processes produce secondary organic aerosols (SOA) that are hygroscopic in
684 composition. The N_{WIBS} is bimodal with the morning peak at 8 am, reflecting rush hour
685 emissions whose particles grow into the size range of the WIBS and then the second maximum
686 at 6 pm as the SOA grow to measurable sizes. The diel trends in the FAP concentrations are
687 not correlated with the CN, CCN or N_{WIBS} as they remain fairly constant throughout the
688 daylight hours but then rapidly increase to their maximum value that extends from midnight
689 until 6 am.

690 The FAP are classified according to the wavelength at which they were excited and wavelength
691 at which they emitted fluorescence. These types have been categorized as A, B, C, AB, AC,
692 BC, and ABC. In the current study the types A, B, C and ABC all had average concentrations
693 during the daylight hours of about 1000 L^{-1} while the other three types were much lower in
694 concentration; however, only the type ABC showed the rapid increase in concentration, to
695 almost 5000 L^{-1}, between midnight and 6 am.

696 Independent measurements using fluorescent microscopy of spores captured on substrates were
697 made during the same time period. Although more than 20 species of spores were identified
698 with this technique, the fungi Basidiospores and Ascospores ~~Basidiomycetes and Ascomycetes~~
699 were not only the most predominant, but they were also the spores that followed an almost
700 identical diel trend as the type ABC FAP, i.e. remaining nearly constant in concentration during
701 the daylight hours then increasing in the evening to their maxima between midnight and 6 am
702 with larger shifts of EOD with increase of RH.

703 The other environmental parameters that also correlated significantly with the temporal trends
704 in fungal spores and FAP were the relative humidity (RH) and the wind speed. As the RH
705 began to increase in the late afternoon, the spore counts and FAP concentrations began
706 increasing as well. A comparison of RH with FAP concentrations indicates that the FAP

concentrations begin increasing above an RH threshold of about 80%. Spores are released by a number of species of fungi when the RH increases, as has been well documented in other studies (Quintero et al., 2010). Hence, the relationship between RH, Basidiomycetes and Ascomycetes and the type ABC FAP has been clearly established.

Three additional properties of the FAP were extracted from the WIBS measurements that provided indirect but complementary information that showed how the type ABC particles were related to the Basidiomycetes and Ascomycetes: 1) the size distribution, 2) the asphericity and 3) the excitation and emission sensitivity parameters. The type ABC particles during the high RH periods had much higher concentrations of particles larger than 2 µm when compared to the size distributions of these particles in the daylight hours. Secondly, the asphericity increased during the high type ABC concentration period. Thirdly, excitation sensitivity parameters increased during this same period. While not quantitative, these three parameters confirmed that the particles whose concentrations were increasing had different properties than during other periods of the day.

The trend in the CCN concentration was not directly correlated with the FAP, so we cannot conclude that bioaerosols are a potential source of cloud forming particles. In addition, the FAP concentrations were less than 10% of CCN concentrations, so even if some FAP are potential CCN, the clouds that develop over the island are more likely formed from marine aerosols rather than locally produced fungal spores.

The results from this pilot study have provided strong motivation for longer term measurements that will expand the database of aerosol particle properties in a tropical, urban area. The detailed information on fungal spores in this region, in comparison with the multi-parameter data available from the WIBS, will improve our ability to interpret these measurements of FAP and apply this knowledge to data sets acquired in other parts of the world.

Data availability

Data used to support the findings in this study have been uploaded and are publicly available via Mendeley at https://data.mendeley.com/datasets/t26dctfk7t/1 (Sarangi et al., 2021).

Author Contribution

BS designed the study in consultation with OLMB and performed the measurements. BBR performed the measurements of fungal spores and pollen concentrations. DB and BS performed

the analysis, interpreted the results and wrote the paper with contributions from OLMB and BBR.

Acknowledgements

This research was supported by NSF MRI grant (1829297) and NSF EAR Grant (1331841). The authors acknowledge the Droplet Measurement Technologies, Inc., Boulder, Colorado for providing training on instruments that are part of the NSF MRI project. The authors gratefully acknowledge the NOAA Air Resources Laboratory (ARL) for the provision of the HYSPLIT transport model (http://www.ready.noaa.gov).

Reference

Allan, J. D., Baumgardner, D., Raga, G. B., Mayol-Bracero, O. L., Morales-García, F., García-García, F., Montero-Martínez, G., Borrmann, S., Schneider, J., Mertes, S., Walter, S., Gysel, M., Dusek, U., Frank, G. P. and Krämer, M.: Clouds and aerosols in Puerto Rico - A new evaluation, Atmos. Chem. Phys., 8, 1293–1309, doi:10.5194/acp-8-1293-2008, 2008.

Baumgardner, D., Raga, G. B. and Muhlia, A.: Evidence for the formation of CCN by photochemical processes in Mexico City, Atmos. Environ., 38(3), 357–367, doi:10.1016/j.atmosenv.2003.10.008, 2004.

Calvo, A. I., Baumgardner, D., Castro, A., Fernández-González, D., Vega-Maray, A. M., Valencia-Barrera, R. M., Oduber, F., Blanco-Alegre, C. and Fraile, R.: Daily behavior of urban Fluorescing Aerosol Particles in northwest Spain, Atmos. Environ., 184, 267-277, doi:10.1016/j.atmosenv.2018.04.027, 2018.

Caulton E and Lacey M.: Airborne Pollens and Spores. A Guide to Trapping and Counting, 1st ed., British Aerobiology Federation (BAF) Publishers, 1995.

Chi, M. C. and Li, C. S.: Fluorochrome in monitoring atmospheric bioaerosols and correlations with meteorological factors and air pollutants, Aerosol Sci. Technol., 41, 672-678, doi:10.1080/02786820701383181, 2007.

Cziczo, D. J., Thomson, D. S., Thompson, T. L., DeMott, P. J. and Murphy, D. M.: Particle analysis by laser mass spectrometry (PALMS) studies of ice nuclei and other low number density particles, Int. J. Mass Spectrom., 258, 21-29, doi:10.1016/j.ijms.2006.05.013, 2006.

766 Drewnick, F., Dall'Osto, M. and Harrison, R.: Characterization of aerosol particles from grass
767 mowing by joint deployment of ToF-AMS and ATOFMS instruments, Atmos. Environ.,
768 42(13), 3006–3017, doi:10.1016/j.atmosenv.2007.12.047, 2008.

769 Duan, J., Chen, Y. and Guo, X.: Characteristics of aerosol activation efficiency and aerosol and
770 CCN vertical distributions in North China, Acta Meteorol. Sin., 26, 579–596,
771 doi:10.1007/s13351-012-0504-6, 2012.

772 Fennelly, M. J., Sewell, G., Prentice, M. B., O'Connor, D. J., and Sodeau, J. R.: The Use of
773 Real-Time Fluorescence Instrumentation to Monitor Ambient Primary Biological Aerosol
774 Particles (PBAP), Atmosphere, 9, 1–39, https://doi.org/10.3390/atmos9010001, 2017.

775 Fröhlich-Nowoisky, J., Kampf, C. J., Weber, B., Huffman, J. A., Pöhlker, C., Andreae, M. O.,
776 Lang-Yona, N., Burrows, S. M., Gunthe, S. S., Elbert, W., Su, H., Hoor, P., Thines, E.,
777 Hoffmann, T., Després, V. R. and Pöschl, U.: Bioaerosols in the Earth system: Climate, health,
778 and ecosystem interactions, Atmos. Res., 182, 346-376, doi:10.1016/j.atmosres.2016.07.018,
779 2016.

780

781 Gabey, A. M.: Laboratory and field characterization of fluorescent and primary biological
782 aerosol particles, Ph.D. thesis, University of Manchester, England, 2011.

783 Gabey, A. M., Gallagher, M. W., Whitehead, J., Dorsey, J. R., Kaye, P. H., and Stanley, W.
784 R.: Measurements and comparison of primary biological aerosol above and below a tropical
785 forest canopy using a dual channel fluorescence spectrometer, Atmos. Chem. Phys., 10, 4453–
786 4466, doi:10.5194/acp-10-4453-2010, 2010.

787 Gabey, A. M., Vaitilingom, M., Freney, E., Boulon, J., Sellegri, K., Gallagher, M. W.,
788 Crawford, I. P., Robinson, N. H., Stanley, W. R., and Kaye, P. H.: Observations of fluorescent
789 and biological aerosol at a high-altitude site in central France, Atmos. Chem. Phys., 13, 7415–
790 7428, https://doi.org/10.5194/acp-13-7415-2013, 2013.

791 Gioda, A., Mayol-Bracero, O. L., Scatena, F. N., Weathers, K. C., Mateus, V. L. and
792 McDowell, W. H.: Chemical constituents in clouds and rainwater in the Puerto Rican
793 rainforest: Potential sources and seasonal drivers, Atmos. Environ., 68, 208-220,
794 doi:10.1016/j.atmosenv.2012.11.017, 2013.

795 Gosselin, M. I., Rathnayake, C. M., Crawford, I., Pöhlker, C., Fröhlich-Nowoisky, J., Schmer,
796 B., Després, V. R., Engling, G., Gallagher, M., Stone, E., Pöschl, U., and Huffman, J. A.:
797 Fluorescent bioaerosol particle, molecular tracer, and fungal spore concentrations during dry
798 and rainy periods in a semi-arid forest, Atmos. Chem. Phys., 16, 15165–15184,
799 https://doi.org/10.5194/acp-16-15165-2016, 2016.

800 Healy, D. A., Huffman, J. A., O'Connor, D. J., Pöhlker, C., Pöschl, U., and Sodeau, J. R.:
801 Ambient measurements of biological aerosol particles near Killarney, Ireland: a comparison
802 between real-time fluorescence and microscopy techniques, Atmos. Chem. Phys., 14, 8055–
803 8069, https://doi.org/10.5194/acp-14-8055-2014, 2014.

804 Hernandez, M., Perring, A. E., McCabe, K., Kok, G., Granger, G., and Baumgardner, D.:
805 Chamber catalogues of optical and fluorescent signatures distinguish bioaerosol classes,
806 Atmos. Meas. Tech., 9, 3283–3292, https://doi.org/10.5194/amt-9-3283-2016, 2016.

807 Ho, J., Spence, M., and Hairston, P.: Measurement of Biological Aerosol with a Fluorescent
808 Aerodynamic Particle Sizer (FLAPS): Correlation of Optical Data with Biological Data,
809 Aerobiologia, 15, 281, https://doi.org/10.1023/A:1007647522397, 1999.

810 Hoose, C., Kristjánsson, J. E. and Burrows, S. M.: How important is biological ice nucleation
811 in clouds on a global scale?, Environ. Res. Lett., 5(2), 024009, doi:10.1088/1748-
812 9326/5/2/024009, 2010.

813

814 Huffman, J. A. and Santarpia, J. L.: Online techniques for quantification and characterization
815 of biological aerosol, in: Microbiology of Aerosols, edited by: Delort, A. M. and Amato, P.,
816 Wiley, Hoboken, NJ, chap. 1.4, 2017.

817 Jaenicke, R.: Abundance of cellular material and proteins in the atmosphere, Science (80-.).,
818 308(5718), 73. doi:10.1126/science.1106335, 2005.

819

820 Kaye, P. H., Stanley, W. R., Hirst, E., Foot, E. V., Baxter, K. L., and Barrington, S. J.: Single
821 particle multichannel bio-aerosol fluorescence sensor, Opt. Express, 13, 3583-3593, 2005.

822 Kaye, P. H., Aptowicz, K., Chang, R. K., Foot, V., and Videen, G.: Angularly resolved elastic
823 scattering from airborne particles - Potential for characterizing, classifying, and identifying
824 individual aerosol particles, Opt. Biol. Part., 238, 31–61, 2007.

Kulkarni, P., Baron, P. A. and Willeke, K.: Aerosol Measurement: Principles, Techniques, and Applications: Third Edition., 2011.

Kunert, A. T., Pöhlker, M. L., Tang, K., Krevert, C. S., Wieder, C., Speth, K. R., Hanson, L. E., Morris, C. E., Schmale, D. G., Pöschl, U. and Fröhlich-Nowoisky, J.: Macromolecular fungal ice nuclei in Fusarium: Effects of physical and chemical processing, Biogeosciences, 16(23), 4647-4659, doi:10.5194/bg-16-4647-2019, 2019.

Lewis, L. M., and Coauthors, 2019: Characterizing environmental asthma triggers and healthcare use patterns in Puerto Rico. J. Asthma, ; 57(8): 886–897, https://doi.org/10.1080/02770903.2019.1612907.

Möhler, O., DeMott, P. J., Vali, G., and Levin, Z.: Microbiology and atmospheric processes: the role of biological particles in cloud physics, Biogeosciences, 4, 1059–1071, doi:10.5194/bg-4-10592007, 2007.

Oliveira, M., Ribeiro, H. and Abreu, I.: Annual variation of fungal spores in atmosphere of Porto: 2003, Ann. Agric. Environ. Med., 12(2), 309-315, 2005.

Ortiz-Martínez, M. G., Rodríguez-Cotto, R. I., Ortiz-Rivera, M. A., Pluguez-Turull, C. W. and Jiménez-Vélez, B. D.: Linking Endotoxins, African Dust PM_{10} and Asthma in an Urban and Rural Environment of Puerto Rico, Mediators Inflamm., 2015, 784212, doi:10.1155/2015/784212, 2015.

Perring, A. E., Schwarz, J. P., Baumgardner, D., Hernandez, M. T., Spracklen, D. V., Heald, C. L., Gao, R. S., Kok, G., McMeeking, G. R., McQuaid, J. B., and Fahey, D. W.: Airborne observations of regional variation in fluorescent aerosol across the United States, J. Geophys. Res.-Atmos., 120, 1153–1170, https://doi.org/10.1002/2014JD022495, 2015.

Pope, F. D.: Pollen grains are efficient cloud condensation nuclei, Environ. Res. Lett., 5, 044015, doi:10.1088/17489326/5/4/044015, 2010.

Quintero, E., Rivera-Mariani, F. and Bolaños-Rosero, B.: Analysis of environmental factors and their effects on fungal spores in the atmosphere of a tropical urban area (San Juan, Puerto Rico), Aerobiologia (Bologna)., 26, 113–124, doi:10.1007/s10453-009-9148-0, 2010.

Raga, G. B., Baumgardner, D. and Mayol-Bracero, O. L.: History of aerosol-cloud interactions derived from observations in mountaintop clouds in Puerto Rico, Aerosol Air Qual. Res., 16, 674–688, doi:10.4209/aaqr.2015.05.0359, 2016.

Formatted: Space After: 8 pt, Line spacing: 1.5 lines

Roberts, G. C. and Nenes, A.: A Continuous-Flow Streamwise Thermal-Gradient CCN Chamber for Atmospheric Measurements, Aerosol Sci. Technol., 39, 206–221, 2005.

Rose, D., Gunthe, S. S., Mikhailov, E., Frank, G. P., Dusek, U., Andreae, M. O., and Pöschl, U.: Calibration and measurement uncertainties of a continuous-flow cloud condensation nuclei counter (DMT-CCNC): CCN activation of ammonium sulfate and sodium chloride aerosol particles in theory and experiment, Atmos. Chem. Phys., 8, 1153–1179, https://doi.org/10.5194/acp-8-1153-2008, 2008.

Rivera-Mariani, F. E., Nazario-Jiménez, S., López-Malpica, F. and Bolaños-Rosero, B.: Sensitization to airborne ascospores, basidiospores, and fungal fragments in allergic rhinitis and asthmatic subjects in San Juan, Puerto Rico, Int. Arch. Allergy Immunol., 155, 322-334, doi:10.1159/000321610, 2011.

Rivera-Mariani, F. E., Almaguer, M., Aira, M. J. and Bolaños-Rosero, B.: Comparison of atmospheric fungal spore concentrations between two main cities in the Caribbean basin, P. R. Health Sci. J., 39(3), 235–242, 2020.

Sarangi, B., Baumgardner, D., Bolaños-Rosero, B. and Mayol-Bracero, O. L.: Dataset to: Measurement Report: An Exploratory Study of Fluorescence and CCN Activity of Urban Aerosols in San Juan, Puerto Rico, Mendeley Data, Version 1, doi:10.17632/t26dctfk7t.1, 2021.

Savage, N. J., Krentz, C. E., Könemann, T., Han, T. T., Mainelis, G., Pöhlker, C. and Alex Huffman, J.: Systematic characterization and fluorescence threshold strategies for the wideband integrated bioaerosol sensor (WIBS) using size-resolved biological and interfering particles, Atmos. Meas. Tech., 10, 4279–4302, doi:10.5194/amt-10-4279-2017, 2017.

Spiegel, J. K., Buchmann, N., Mayol-Bracero, O. L., Cuadra-Rodriguez, L. A., Valle Díaz, C. J., Prather, K. A., Mertes, S. and Eugster, W.: Do Cloud Properties in a Puerto Rican Tropical Montane Cloud Forest Depend on Occurrence of Long-Range Transported African Dust?, Pure Appl. Geophys., 171(9), 2443–2459, https://doi.org/10.1007/s00024-014-0830-y, 2014.

Stanley, W. R., Kaye, P. H., Foot, V. E., Barrington, S. J., Gallagher, M. and Gabey, A.: Continuous bioaerosol monitoring in a tropical environment using a UV fluorescence particle spectrometer, Atmos. Sci. Lett., 12, 195–199, doi:10.1002/asl.310, 2011.

Stocker, T.F., Qin, D., Plattner, G.-K., Tignor, M., Allen, S.K., Boschung, J., Nauels, A., Xia, Y., Bex, V., Midgley, P.M., 2013. IPCC, 2013: climate change 2013: the physical science basis.

Contribution of working group I to the fifth assessment report of the intergovernmental panel on climate change. IPCC, 2013. Cambridge University Press, Cambridge, United Kingdom and New York, NY, USA, p. 1535. Stommel, E.W., Fiel

Stolzenburg, M. R. and McMurry, P. H.: An Ultrafine Aerosol Condensation Nucleus Counter, Aerosol Sci. Tech., 14, 48–65, 1991.

Toprak, E. and Schnaiter, M.: Fluorescent biological aerosol particles measured with the Waveband Integrated Bioaerosol Sensor WIBS-4: laboratory tests combined with a one year field study, Atmos. Chem. Phys., 13, 225–243, https://doi.org/10.5194/acp-13-225-2013, 2013.

Torres-Delgado, E., Baumgardner, D., and Mayol-Bracero, O. L.: Measurement Report: Impact of African Aerosol Particles on Cloud Evolution in a Tropical Montane Cloud Forest in the Caribbean, Atmos. Chem. Phys. Discuss. [preprint], https://doi.org/10.5194/acp-2021-88, in review, 2021.

Toro-Heredia, J., Jirau-Colón, H. and Jiménez-Vélez, B. D.: Linking PM2.5 organic constituents, relative toxicity and health effects in Puerto Rico, Environ. Challenges, 5, 100350, doi:10.1016/j.envc.2021.100350, 2021.

Twohy, C. H., McMeeking, G. R., DeMott, P. J., McCluskey, C. S., Hill, T. C. J., Burrows, S. M., Kulkarni, G. R., Tanarhte, M., Kafle, D. N., and Toohey, D. W.: Abundance of fluorescent biological aerosol particles at temperatures conducive to the formation of mixed-phase and cirrus clouds, Atmos. Chem. Phys., 16, 8205–8225, https://doi.org/10.5194/acp-16-8205-2016, 2016.

Valle-Díaz, C. J., Torres-Delgado, E., Colón-Santos, S. M., Lee, T., Collett, J. L., McDowell, W. H., & Mayol-Bracero, O. L.: Impact of long-range transported african dust on cloud water chemistry at a tropical montane cloud forest in Northeastern Puerto Rico. Aerosol and Air Quality Research, 16(3), 653–664. doi.org/10.4209/aaqr.2015.05.0320, 2016.

Velázquez-Lozada, A., Gonza´lez, J. E., and Winter, A.: Urban heat islands effect analysis for San Juan, Puerto Rico. Atmospheric Environment, 40, 1731–1741, 2006.

916 Uin, J.: Ultra-High Sensitivity Aerosol Spectrometer (UHSAS) instrument handbook. ARM Tech. Rep.
917 DOE/SCARM-TR-163, USA, 17 pp., doi.org/10.2172/1251410, 2016.

918 Zhang, M., Khaled, A., Amato, P., Delort, A.-M., and Ervens, B.: Sensitivities to biological
919 aerosol particle properties and ageing processes: potential implications for aerosol–cloud
920 interactions and optical properties, Atmos. Chem. Phys., 21, 3699–3724,
921 https://doi.org/10.5194/acp-21-3699-2021, 2021.

922

923